

Deposition of model chains on surfaces: anomalous relation between flux and stability

Pritam Kumar Jana^{1, a)} and Andreas Heuer^{2, b)}

¹⁾ *Westfälische Wilhelms-Universität Münster, Institut für Physikalische Chemie, Corrensstr. 28/30, 48149 Münster, Germany*

²⁾ *Westfälische Wilhelms-Universität Münster, Institut für Physikalische Chemie, Corrensstr. 28/30, 48149 Münster, Germany*

(Dated: 19 June 2018)

Model chains are studied via Monte Carlo simulations which are deposited with a fixed flux on a substrate. They may represent, e.g., stiff lipophilic chains with an head group and tail groups mimicking the alkyl chain. After some subsequent fixed simulation time we determine the final energy as a function of flux and temperature. Surprisingly, in some range of temperature and flux the final energy increases with decreasing flux. The physical origin of this counterintuitive observation is elucidated. In contrast, when performing equivalent cooling experiments no such anomaly is observed. Furthermore, it is elaborated whether flux experiments give rise to configurations with lower energies as compared to cooling experiments. These results are related to recent experiments by the Ediger group where very stable configurations of glass-forming systems have been generated via flux experiments.

^{a)}Electronic mail: pjana_01@uni-muenster.de

^{b)}Electronic mail: andheuer@uni-muenster.de

I. INTRODUCTION

The growth behavior of molecules, adsorbed on surfaces, has been studied extensively¹⁻⁷. This class of experiments can be guided by different key questions. (1) Using prepatterned surfaces the adsorbed molecules may adopt the same prepatterned structure. In this way one can tune the structure formation of molecules with interesting functions^{2,8-10}. The ability to inherit the underlying structure to the adsorbed molecules has been also analysed from a theoretical perspective; see, Refs. e.g.¹¹⁻¹³ (2) From practical perspective one may optimize the properties of these thin film devices. This may be relevant for field effect transistors¹⁴⁻¹⁸, organic light-emitting diodes¹⁹⁻²¹, or, more generally, opto-electronics^{19,22-24}. (3) Using anisotropic molecules one may want to generate directional order of the molecules on the surface. This order effect, already present for molecules with a large aspect ratio²⁵⁻²⁷, become particularly pronounced for oligomers or polymers. Electronic properties of organic molecular semiconductors can be finely tuned by modifying the chemical structure of their constituting molecules²⁸. Recently it has been shown that also lipophilic alkane-chains with nucleobases as the respective headgroups display highly ordered structures. This specific systems may also be used as the basis of electronics²⁹. (4) By the adsorption of the molecules on a substrate, which was cooled below the glass transition temperature of this system, Ediger and coworkers managed to generate glassy films with an enthalpy which is lower than the enthalpy obtained after cooling a bulk sample in its glassy state³⁰. It was shown that in agreement with expectation the resulting enthalpy was correlated with the applied flux: the smaller the flux the lower the resulting enthalpy. One may generally ask, whether for all systems the enthalpy monotonously depends on the chosen flux.

Inspired by the major interest in the ordering process of anisotropic molecules on surface we specifically discuss this question for stiff oligomers, containing a headgroup and a small tail. For a theoretical analysis of molecular systems on surfaces one often resorts to lattice-gas models due to its simplicity; see, Refs. e.g.,³¹⁻³³. As a minimum system we consider straight trimers on a quadratic lattice.

The general setup of the simulation is shown in Fig.1. We start with a time period during which N chains are deposited on a surface with constant flux at some fixed temperature T . In the subsequent evolution period t_{sim} the system evolves further without the adsorption of additional molecules. At the end of the simulation we record the potential energy as a

measure of the degree of equilibration. At very low temperatures one may expect that the system cannot reach its equilibrium state during t_{sim} . Intuitively, one might expect that for high flux and low temperature the chains form some disordered high-energy configuration during the first time interval which are stabilized by the immediate arrival of new chains. So, the general expectation is that the final state has a higher energy for higher initial flux, though there will be some aging during the evolution period t_{sim} . In contrast, for small flux unfavorable configurations have sufficient time to dissolve so that the final configuration might typically correspond to a low-energy structure.

For comparison we also perform simulations where the initial deposition protocol is substituted by a cooling protocol as also sketched in Fig.1. Starting with an equilibrium configuration of all N chains at a high temperature we study the final energy in dependence on the cooling rate. Here the analogous argument should hold: the slower the schedule of cooling down, the lower the resulting energy³⁴. This effect is the basis of the well-known simulated annealing technique to find low-energy states³⁵.

Here we show that for the chosen model system the flux simulations do not fulfill the general expectation as formulated above. Rather for some temperature regime we find a surprising effect that upon decreasing flux the resulting potential energy increases. Furthermore we show that apart from this specific parameter regime flux simulations seem to be more efficient to find low-energy configurations as compared to cooling simulations. The paper is organized as follows: in Sec. II and Sec. III we describe the model and simulation details, respectively, whereas in Sec. IV the results and the explanation of our observation for the two different approaches to the final system parameters N (number of chains) and T (temperature) are presented, i.e. either by successive adsorption of chains at fixed temperature or by a temperature decrease at fixed number of chains. Finally, we summarize in Sec. V.

II. MODEL

In our model system we consider $N=200$ trimers on a square lattice of length $L = 120$ with periodic boundary conditions. Each trimer consists of one head group (H) and two tail groups (T) and is chosen to be rigid. Each monomer occupies one site of the lattice and the trimers can be arranged along both axes. Naturally, two chains cannot cross each

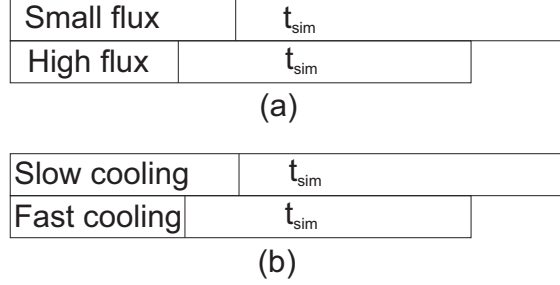


FIG. 1. Schematic presentation of the set-up of the different simulations.

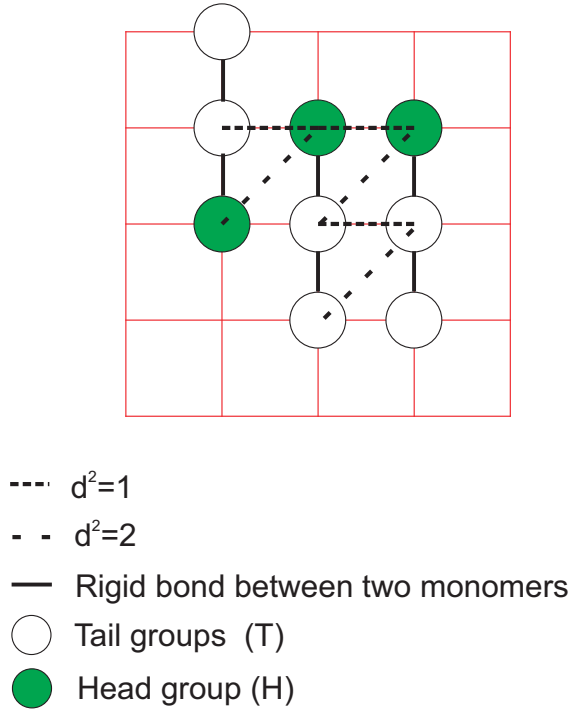
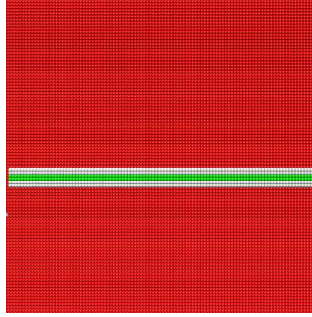
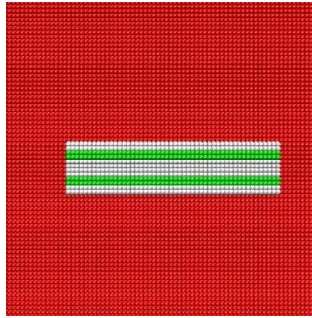


FIG. 2. The model system, consisting of trimers.

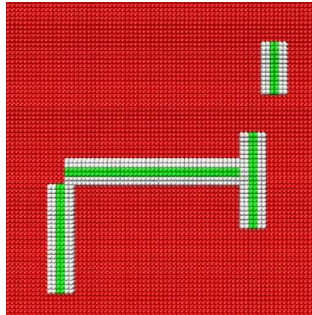
other. The six different types of nearest-neighbor interaction energies between monomers belonging to different molecules are denoted u_{ij_1} , u_{ij_2} with $i, j \in \{H, T\}$. The index '1' and '2' indicates the squared distance between the respective monomers; see Fig. 2. There is the largest interaction between head-groups (HH), in order to guarantee local clustering of them. Furthermore, the tail groups of adjacent chains also attract each other (TT). For alkyl chains this interaction is of van der waals type. The specific energies for the present simulation are listed in Tab. I, given in dimensionless units. Later on it will become clear that the key results of this work do not depend on the specific choice of the interaction parameters as long as the head groups are interacting most strongly and the tail groups



(a)



(b)



(c)

FIG. 3. (a) The ordered structure (O1), (b) The ordered structure O2, and (c) The disordered structures (DO). Different arrangement of the rod like linear trimer HTT.

have a weaker but still finite interaction.

For the subsequent discussion we define the two ordered structures O1- and O2- as displayed in Fig. 3, having one or two stripes. The energies are -2.124 and -2.206 per chain, respectively. Structures with more parallel are hardly seen in our simulations. As compared

Pair	Interaction energy	
	$d^2=1$	$d^2=2$
HH	-1.00	-0.10
TT	-0.20	-0.10
HT	0.25	0.03

TABLE I. Interaction energies of the model chains.

to O1- the ordered structure O2- displays additional interactions of the tail groups between both stripes at the expense of one missing interaction of two parallel pairs of chains. Note that the energy contribution of the interaction of the different tail groups is proportional to the length of the structure. As a consequence for smaller values of N ($N \leq 36$) the structure O1- is more favorable than O2. This generic property of the chain model will become important for our later discussion. In particular for high fluxes and/or low temperatures disordered arrangements will prevail, as shown, e.g., in Fig. 3. This specific structure has an energy of -2.082.

III. SIMULATION DETAILS

Monte Carlo simulations, based on the Metropolis criterion, have been performed. In one simulation step all chains, present at that time, are attempted to move. The move class contains a rotational as well as a translational motion. For the rotational motion one randomly selects one of the two end particles and rotates the total chain by 90° around this particle. For the translational motion the chain is shifted by n lattice sites ($n \geq 1$) in the x- or the y-direction. Here we distinguish whether this motion is restricted to a nearest-neighbor site ($n = 1$: local move) or to any site ($n \geq 1$: global move). For most of the results in this work we use global moves. However, we show that the key results are the same for local moves.

As mentioned already in the Introduction the non-equilibrium simulation period either involve a constant flux of particles or a temperature reduction. In the first case one fixes the flux and the temperature. The first time period stops when all N particles are on

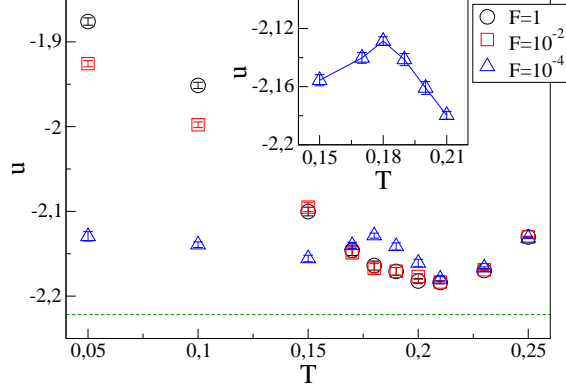


FIG. 4. Variation of u with T at different F . The dotted horizontal line indicates the minimum u of the system. In the inset the data for $F=10^{-4}$ are highlighted. The solid line is a guide to the eyes.

the substrate. In second case one starts with an equilibrated configuration at $T_h = 1$ and reduces the time-dependent temperature $T(t)$ from the initial temperature T_h to the final temperature T_f via

$$T(t) = T_h + \frac{t}{t_{cool}} \times (T_f - T_h). \quad (1)$$

the cooling rate r can be defined as $r = (T_h - T_f)/t_{cool}$. For reasons, discussed below, this type of simulation will be only performed for $T_f = 0.19$.

For one simulation run the resulting potential energy u is defined as the average over the last 25% of the simulation period of length t_{sim} . Furthermore we repeat at least 50 and up to 400 independent simulations, depending on the required statistical accuracy. If not mentioned otherwise, we choose $t_{sim} = 1 \times 10^7$ Monte Carlo steps.

IV. RESULTS AND ANALYSIS

A. Flux simulations

First, we start with the flux simulations. The dependence of the potential energy on flux and temperature, i.e. $u(F, T)$, is shown in Fig. 4. In the limit of high temperatures the time t_{sim} is long enough to generate an equilibrium structure, independent of the initial condition as determined by the chosen flux F . Indeed this independence can be seen for the temperature range $T \geq 0.23$. Naturally, due to the increasing relevance of entropic effects

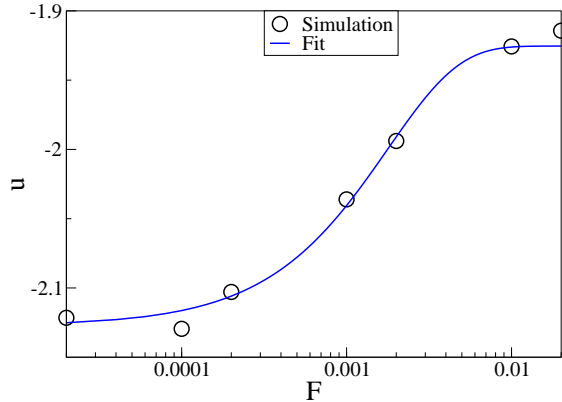


FIG. 5. Variation of u with F at temperature $T=0.05$ for global movement. The solid line is an exponential plot fit $u(F) = a + b \times \exp(-F/F_0)$ with $F_0 = 1.8 \times 10^{-3}$.

with increasing temperature one observes an increase of u . In contrast, in the limit of low temperatures the equilibration time by far exceeds the chosen simulation time t_{sim} . Thus, the final energy still reflects the situation directly after the flux period. For a high flux the time interval between the successive deposition of trimers is so short that by the advent of new chains any temporary disordered structure may be stabilized, giving rise to high-energy structures. Indeed, we see for $T = 0.05$ that within error bars the energy monotonously increases with increasing flux. Interestingly, a closer analysis of the flux-dependence reveals a simple exponential dependence with $F_0 = 1.8 \times 10^{-3}$. See Fig. 5. A closer analysis shows that for $F \ll F_0$ the system is mainly trapped in the O1-structure whereas otherwise the system displays lot of disorder.

Following the arguments for low and high temperatures one would thus expect that for some intermediate temperature a minimum energy u is observed which, furthermore, should increase with increasing flux. As shown in Fig. 4, this simple expectation is not fulfilled. First, the temperature dependence is more complicated. As clearly seen for, e.g., $F = 10^{-4}$ there exists a local maximum of u for $T = 0.18$.

Here we particularly concentrate on the effect of non-monotonous flux dependence for a specific temperature. For the temperature of $T = 0.19$ this effect is explicitly highlighted in Fig. 6 for global as well as local movement. Evidently, one obtains a significantly non-monotonous dependency of energy on flux. For $F \leq 10^{-4}$ some additional mechanism seems to prevent the system to reach the same low-energy configurations as compared to somewhat higher values of the flux. The effect is present for both the global and the local movement.

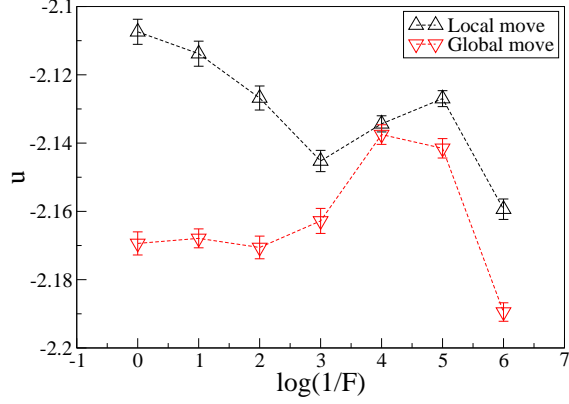


FIG. 6. Variation of u with F at temperature $T=0.19$ for global and local movement. The dashed line is a guide to the eyes.

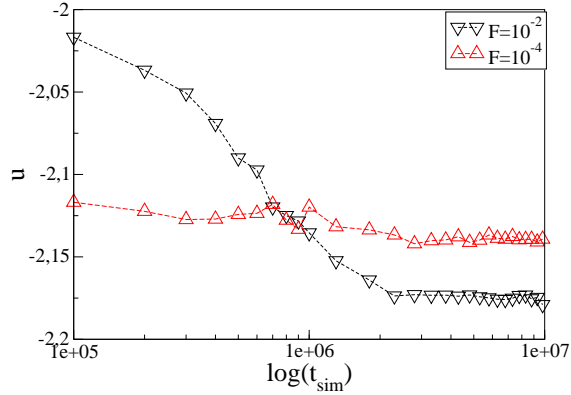


FIG. 7. Variation of u with evolution of time for different values of the flux at temperature $T=0.19$.

As expected, via global moves it is possible to explore the phase space more efficiently, which explains the differences in energy values for the high flux regime. Of course, in the limit of extremely small values of the flux any finite system has to reach its equilibrium structure. This approach to equilibrium starts to become visible for $F < 10^{-5}$; see Fig. 6.

Additional insight into this behavior can be gained by analysing the time-dependence of the energy in the final part of the simulation; see Fig. 7. In the discussion we concentrate on the comparison of $F = 10^{-2}$ and $F = 10^{-4}$. For small values of t_{sim} the configuration, generated with the high flux of $F = 10^{-2}$, is by far more disordered and displays a much higher energy. However, with increasing simulation time a typical high-flux configuration manages to approach structures with energies close to -2.2 whereas the low-flux configuration seems to be stuck in some region of configuration space because the energy hardly decreases

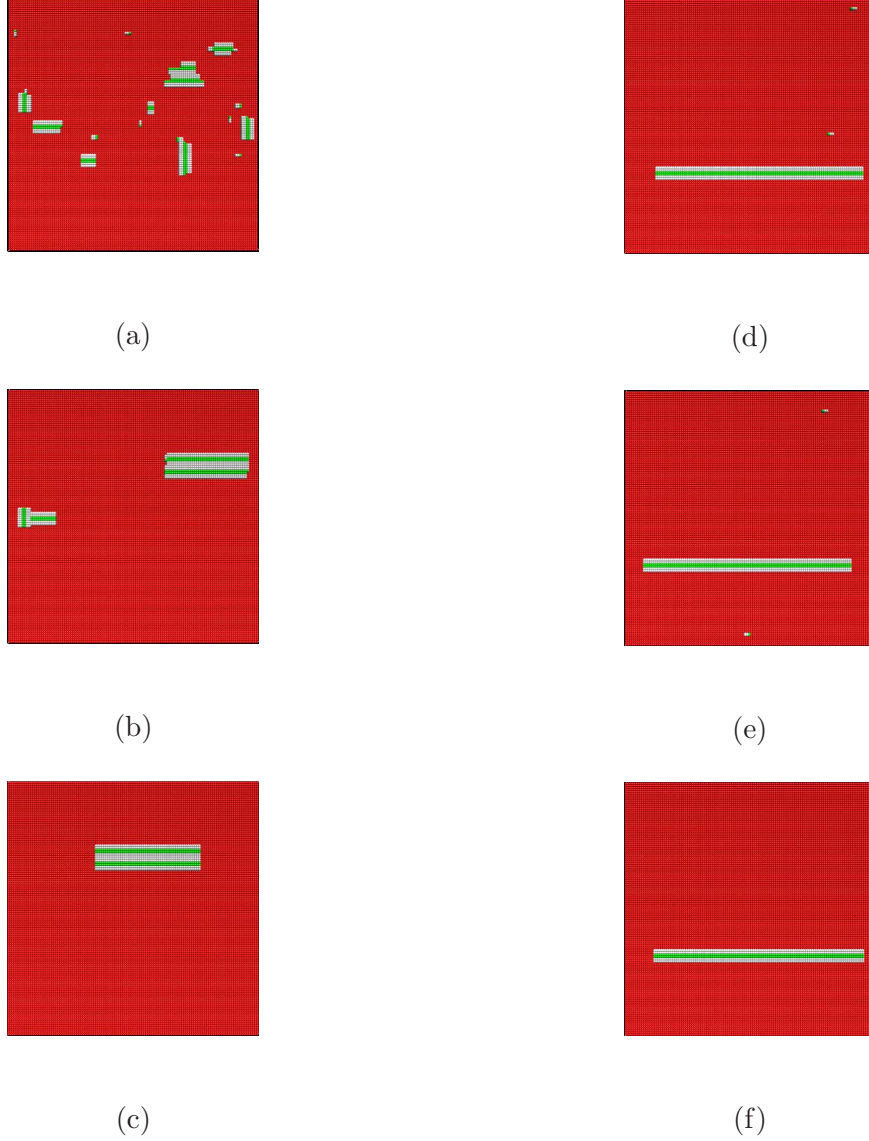


FIG. 8. Mechanism to form the final structure. (a), (b) and (c) are the structures at $t_{sim}=0$, $t_{sim}=1\times 10^6$ and $t_{sim}=1\times 10^7$ for $F=10^{-2}$. (d), (e) and (f) are the structures at $t_{sim}=0$, $t_{sim}=1\times 10^6$ and $t_{sim}=1\times 10^7$ for $F=10^{-4}$.

below -2.13 in the analysed time regime of t_{sim} .

To elucidate the reason of this surprising observation we explicitly monitor the time evolution on a microscopic scale for both flux values as representative examples, respectively; see Fig. 8. For the smaller flux one ends up with the O1-type structure whereas in the other case the final configuration corresponds to the O2-type structure. How to understand this behavior? We assume that 6 trimers are present. The lowest-energy configuration for 6 trimers is shown in Fig. 9(a). As already mentioned above, for a small number of trimers

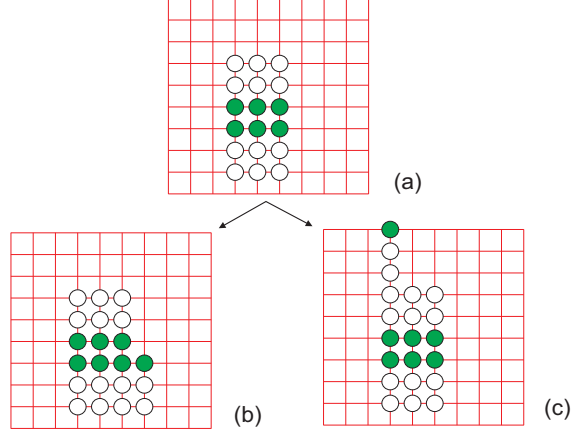


FIG. 9. (a) The lowest-energy configuration for 6 trimers. Addition of one trimer leads to (b) two new TT interactions and one new HH interaction or (c) one new TT interaction.

the O1-configuration has a much lower energy than the O2-configuration. After the next deposition process the new trimer will easily find its way to this cluster via diffusion (local move) or via single hops (global moves). There are, however, several docking options. Two examples are shown in Fig. 9(b) and (c). Energetically favorable is the option (b) where the new trimer is fully bound to an already present trimer. In practice it is likely the new trimer explores several of the available docking options. If sufficient time is given, it is most likely to be found in configuration (b) but in particular for short times after its arrival, configuration (c) can also be realized. Here flux enters into the discussion. With the advent of the next deposited trimer the present configuration may be stabilized and it will become more difficult to change the configuration. Thus, stabilization of configuration (c) is more likely for the high flux as compared to the low flux. This immediately leads to more O2-configurations for a high than for a low flux. Of course, several defects may develop for a high value of the flux as shown in Fig. 8 (a).

The complete qualitative argument for the observed anomalies is schematically summarized in Fig.10. We start with the low-flux case. As discussed before the system may likely end up in an O1-structure because this structure is favorable for a smaller number of trimers. Unfortunately, with an increasing number of trimers this state becomes metastable and the O2-structure becomes the global energy minimum. This barrier is indicated in Fig. 10. Starting from a perfectly ordered O1-structure this transition would involve the successive desorption of 16 trimers (when the 9th pair of trimers is desorbed, the O2-configuration

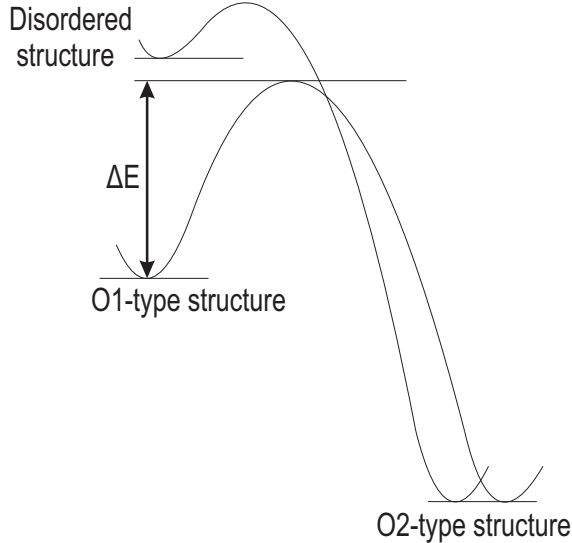


FIG. 10. Schematic presentation of the activation energy for structural rearrangement from Figure 8 (a) (disordered structure) to Figure 8 (c) and from Figure 8 (d) (O1-type structure) to Figure 8 (c).

becomes energetically favorable) from the O1-structure until the system realizes that the O2-structure is energetically favorable. As a consequence neither during the growth period nor during the evolution period t_{sim} the system can surmount the resulting free energy barrier to reach the O2-structure. The situation is different for the high-flux case. During the deposition process it is likely that beyond the O1-structure additional stripes are generated, leading to the O2- or even higher order structures. Additionally, several defects may be present. During the evolution period t_{sim} the different subclusters typically form one big cluster. Furthermore, since it is unlikely that the system is trapped in the O1-configuration it is possible via some minor activated processes to generate an O2-type structure. In any event, the resulting free energy barrier is sufficiently small and can be surmounted during our chosen simulation time t_{sim} .

So far we have analysed the energetic aspects of structure formation. Similarly, one may wonder whether entropic aspects favor either the O1- or the O2-configuration. Naturally, the perfect configurations have the same entropy. At finite temperatures both types of configurations may have some defects. The number of defects with still reasonable energies may be different for both types of configurations. Formally, this can be expressed in terms of an equilibrium entropy. Therefore we have performed long simulations at $T = 0.23$ (using

x	0	4	8	12	16
N_{O1}/N_{O2}	1.1	0.3	0.2	0.1	0.1
$u_{O2} - u_{O1}$	0.0	0.1	0.4	0.6	0.6
$S_{O1} - S_{O2}$	0.1 ± 0.1	-1.5 ± 0.1	-3.6 ± 0.1	-4.5 ± 0.1	-4.8 ± 0.1

TABLE II. Thermodynamic properties of O1- and O2-configurations at temperature $T = 0.23$ for 36 chains using $L = 25$. x : Maximum number of defects for the definition of O1- and O2-configuration. N_{O1}/N_{O2} : Probability ratio of forming an O1- as compared to an O2-structure. $u_{O2} - u_{O1}$: Energy difference between typical O1- and O2-structures. $S_{O1} - S_{O2}$: Entropy difference.

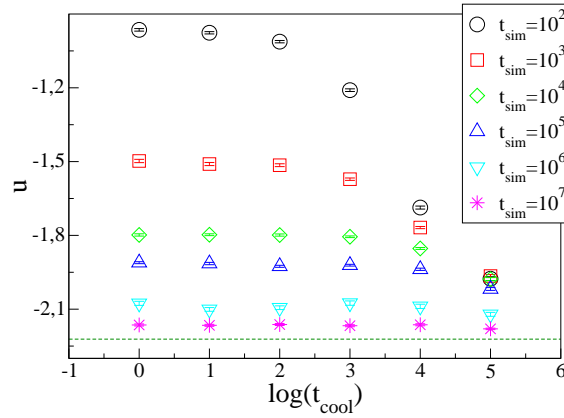
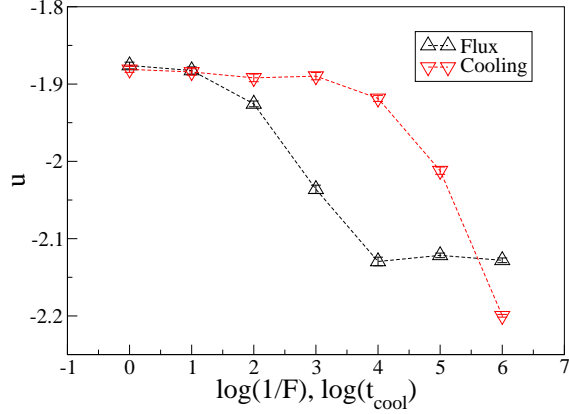
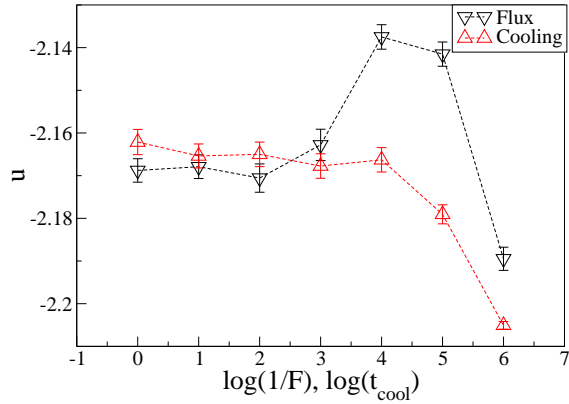


FIG. 11. Change of u with cooling rate for different choices of t_{sim} at $T=0.19$. The dotted horizontal line indicates the minimum u of the system.

$L = 0.25$) where we determined the probability that a O1- or O2-configuration with at most x ($x \in \{0, 4, 8, 12, 16\}$) defects occurs. Using the standard relation $Z = \exp(U - TS)$ we have obtained the relative entropies ($S_{O1} - S_{O2}$) from knowledge of the relative populations (Z_{O1}/Z_{O2}) and the average energies ($u_{O2} - u_{O1}$). For this specific simulation we have used $N = 36$ because for this system size the perfect O1- and O2-structure have nearly identical energies. The results are listed in Tab.II. Indeed one can see that entropically the O2-structure is favored. The entropy difference may thus help to transfer an O1-structure to an O2-structure because of larger attraction basin of the O2-structure.



(a)



(b)

FIG. 12. Comparison of the resulting energy for the flux simulations and the cooling simulations at (a) $T = 0.05$ and (b) $T = 0.19$. The dashed line is a guide to the eyes.

B. Cooling simulations

In the next step, we switch from the deposition to the cooling mechanism to reach the final values of N and T . Choosing a final temperature of $T = 0.19$ we just observe the standard behavior; see Fig. 11. First, shortly after the cooling period is finished the configurations generated with the fastest cooling protocol have the highest energy. Second, after the cooling when the evolution period t_{sim} is finished, the energy still depends in a monotonous way on the initial cooling rate. The difference can be easily rationalized. Since from the very beginning all $N = 200$ chains are present just for entropic reasons the system will not be confined to end up in the O1-structure. Naturally, for given cooling time t_{cool} aging effects

can be only observed if t_{sim} starts to exceed the initial cooling time t_{cool} .

Finally, it may be interesting to compare the degree of equilibration for the flux and the cooling setup. For this purpose we monitor the energy at $T=0.19$ and $T=0.05$ for both scenarios. By matching the respective times of the flux and the cooling period, respectively, we can directly compare the efficiency of both methods to reach structures with lower energies in the low-temperature regime; see Fig. 12. It turns out that for the main part of the parameter regime the flux simulations are more efficient. This effect is particularly pronounced at very low temperatures. Since the cooling simulation starts with all $N = 200$ chains very complex disordered structures may be generated which cannot be dissolved during the simulation. In contrast, due to the gradual increase of the number of molecules in the initial part of the flux simulation this effect seems to be less pronounced. The results are different in the regime where the O1- vs. O2-problem, discussed in this work, becomes relevant. As one can see for $F = 10^{-4}$ and $F = 10^{-5}$ at $T = 0.19$ cooling simulations are more efficient. This effect can easily be explained. In the flux simulations one generates with a high probability O1-configurations which, finally gives rise to somewhat higher energies as compared to the simulations with higher flux. Naturally, this effect does not occur for the cooling simulations because the system starts with a very disordered structure at the starting temperature T_h .

V. SUMMARY AND CONCLUSION

With the help of Monte Carlo simulation we have analyzed the effect of flux and temperature on the behavior of a monolayer film formed by rigid head-tail trimers on the square lattice. Our chosen evolution time t_{sim} was long enough so that for $T \geq 0.23$ the final configuration corresponds to an equilibration configuration, i.e. its energy does not depend on the initialization period. The most interesting temperature regime is slightly below the onset of equilibration. Here we find an increase of the final energy with decreasing flux. On a qualitative level this effect can be understood from the observation that for very low flux the system ends up in a O1-type configuration which for a small number of chains forms the global energy minimum. However, with increasing number of adsorbed chains this global minimum starts to become a local minimum. Then the system is no longer able to escape to the newly developed global minimum, corresponding to the O2-type configuration. In contrast, when replacing the deposition period by a cooling period the expected correlation

between energy and cooling rate is observed.

We would like to note that the same scenario is also obtained for larger chains because this general mechanism works as well. For example we have observed that for a hexamer (one H and five T groups) the energy also displays a maximum as a function of temperature using $F = 10^{-5}$ and $t_{sim} = 5 \times 10^7$. It is observed at $T = 0.25$. In general, the critical temperature range as well as the critical cluster size naturally depends on the potential parameters and the chain length. For example critical cluster size which is $N = 36$ for our standard trimer increases to $N = 60$ for this hexamer.

When the system size is doubled analogous effects are also observed. Indeed, since the mechanism of this anomalous flux dependence is very general, it is not surprising that this phenomenon is robust against variation of system parameters. Of course, going to even much larger values of L , it would be required to increase the number of chains accordingly. Then one would observe several smaller clusters. Their local properties, however, just follow the general mechanisms described in this work.

This work shows that the observation of Ediger and coworkers about the monotonous enthalpy-flux dependence does not hold in general³⁰. Rather for molecules with intrinsic anisotropies a more complex behavior can occur. However, in agreement with these experiments we generally observe that the system generation via deposition can be very efficient to generate low-energy structures if compared with cooling from a high-temperature equilibrium structure.

By the same experimental setup from Ref.³⁰, in principle it may be possible to observe these effects also experimentally for chain molecules, containing a head- and a short tail-region. The only condition is the separation of energy scales of the two types of binding as shown in Fig. 9. The present simulations indicate that the temperature regime for this effect may be sufficiently large. For our specific choice of parameters it is approx. between the temperatures 0.15 and 0.2. In further work it may be helpful to study even simpler model systems where also analytical calculations are possible. Then it may be checked in more detail for which interaction parameters an optimum visibility of this anomalous flux-dependence is possible. This may be helpful for the question for which real-world systems this effect may also be seen experimentally.

VI. ACKNOWLEDGEMENT

We gratefully acknowledge the support by the DFG (SFB 858) and helpful discussions with Mark Ediger and Lifeng Chi as well as her group.

REFERENCES

- ¹T. Michely and J. Krug, *Islands, Mounds and Atoms* (Springer-Verlag, Berlin, 2004).
- ²W. C. Wang, D. Y. Zhong, J. Zhu, F. Kalischewski, R. F. Dou, K. Wedeking, Y. Wang, A. Heuer, H. Fuchs, G. Erker, and L. F. Chi, *Phys. Rev. Lett.* **98**, 225504 (2007).
- ³J. A. Venables and J. H. Harding, *J. Cryst. Growth* **211**, 27 (2000).
- ⁴G. Haas, A. Menck, H. Brune, J. V. Barth, J. A. Venables, and K. Kern, *Phys. Rev. B* **61**, 11105 (2000).
- ⁵R. Vardavas, C. Ratsch, and R. E. Caflisch, *Surf. Sci.* **569**, 185 (2004).
- ⁶L. Nurminen, A. Kuronen, and K. Kaski, *Phys. Rev. B* **63**, 035407 (2000).
- ⁷R. F. Sabiryanov, M. I. Larsson, K. J. Cho, W. D. Nix, and B. M. Clemens, *Phys. Rev. B* **67**, 125412 (2003).
- ⁸Z. Zhong and G. Bauer, *Appl. Phys. Lett.* **84**, 1922 (2004).
- ⁹A. L. Briseno, J. Aizenberg, Y.-J. Han, R. A. Penkala, H. Moon, A. J. Lovinger, C. Kloc, and Z. Bao, *J. Am. Chem. Soc.* **127**, 12164 (2005).
- ¹⁰B. Dong, D. Y. Zhong, L. F. Chi, and H. Fuchs, *Adv. Mater.* **17**, 2736 (2005).
- ¹¹F. Kalischewski, J. Zhu, and A. Heuer, *Phys. Rev. B* **78**, 155401 (2008).
- ¹²F. Kalischewski and A. Heuer, *Phys. Rev. B* **80**, 155421 (2009).
- ¹³F. Lied, T. Mues, W. Wang, L. Chi, and A. Heuer, *J. Chem. Phys.* **136**, 024704 (2012).
- ¹⁴A. Tsumura, H. Koezuka, and T. Ando, *Appl. Phys. Lett.* **49**, 1210 (1986).
- ¹⁵J. H. Burroughes, C. A. Jones, and R. H. Friend, *Nature* **335**, 137 (1988).
- ¹⁶A. Assadi, C. Svensson, M. Willander, and O. Inganäs, *Appl. Phys. Lett.* **53**, 195 (1988).
- ¹⁷J. Paloheimo, P. Kuivalainen, H. Stubb, E. Vuorimaa, and P. Yli-Lahti, *Appl. Phys. Lett.* **56**, 1157 (1990).
- ¹⁸G. Horowitz, D. Fichou, X. Peng, Z. Xu, and F. Garnier, *Solid State Commun.* **72**, 381 (1989).

- ¹⁹J. H. Burroughes, D. D. C. Bradley, A. R. Brown, R. N. Marks, K. Mackay, R. H. Friend, P. L. Burns, and A. B. Holmes, *Nature* **347**, 539 (1990).
- ²⁰Y. Ohmori, M. Uchida, K. Muro, and K. Yoshino, *Solid State Commun.* **80**, 605 (1991).
- ²¹D. Braun and A. J. Heeger, *Appl. Phys. Lett.* **58**, 1982 (1991).
- ²²G. Yu, J. Gao, J. C. Hummelen, F. Wudl, and A. J. Heeger, *Science* **270**, 1789 (1995).
- ²³H. Sirringhaus, N. Tessler, and R. H. Friend, *Science* **280**, 1741 (1998).
- ²⁴J.-S. Yang and T. M. Swager, *J. Am. Chem. Soc.* **120**, 11864 (1998).
- ²⁵S. F. Hopp and A. Heuer, *J. Chem. Phys.* **136**, 154106 (Apr 2012).
- ²⁶L. Bellier-Castella, D. Caprion, and J.-P. Ryckaert, *J. Chem. Phys.* **121**, 4874 (2004).
- ²⁷V. Palermo, F. Biscarini, and C. Zannoni, *Phys. Rev. E* **57**, 2519 (1998).
- ²⁸F. Garnier, A. Yassar, R. Hajlaoui, G. Horowitz, F. Deloffre, B. Servet, S. Ries, and P. Alnot, *J. Am. Chem. Soc.* **115**, 8716 (1993).
- ²⁹Q. Zeng, C. Wang, B. Zhang, S. Xu, P. Wu, X. Qiu, and C. Bai, *J. Indian Chem. Soc.* **77**, 599 (2000).
- ³⁰K. L. Kearns, S. F. Swallen, M. D. Ediger, T. Wu, Y. Sun, and L. Yu, *J. Phys. Chem. B* **112**, 4934 (2008).
- ³¹F. Romá, A. J. Ramirez-Pastor, and J. L. Riccardo, *Phys. Rev. B* **68**, 205407 (2003).
- ³²F. Romá, A. J. Ramirez-Pastor, and J. L. Riccardo, *Phys. Rev. B* **72**, 035444 (2005).
- ³³W. Rżysko and M. Borówko, *J. Chem. Phys.* **135**, 194702 (2011).
- ³⁴S. Sastry, P. G. Debenedetti, and F. H. Stillinger, *Nature* **393**, 554 (1998).
- ³⁵S. Kirkpatrick, C. D. Gelatt Jr., and M. P. Vecchi, *Science* **220**, 671 (1983).